Bond valence analysis of reverse Monte Carlo produced structural models; a way to understand ion conduction in glasses

2005 J. Phys.: Condens. Matter 17 S87

(http://iopscience.iop.org/0953-8984/17/5/010)

INSTITUTE OF PHYSICS PUBLISHING JOURNAL OF PHYSICS: CONDENSED MATTER

J. Phys.: Condens. Matter **17** (2005) S87–S101 doi:10.1088/0953-8984/17/5/010

Bond valence analysis of reverse Monte Carlo produced structural models; a way to understand ion conduction in glasses

Stefan Adams[1] **and Jan Swenson**[2]

[1] GZG, Abteilung Kristallographie, Universität Göttingen, Goldschmidtstraße 1, D-37077 Göttingen, Germany
[2] Department of Applied Physics, Chalmers University of Technology, S-412 96 Göteborg, Sweden

Received 3 November 2004, in final form 3 November 2004
Published 21 January 2005
Online at stacks.iop.org/JPhysCM/17/S87

Abstract

Reverse Monte Carlo (RMC) modelling is now widely used for obtaining structural models of amorphous materials that are in quantitative agreement with available experimental structure data. In the case of ion conducting glasses it has been possible to determine the distribution and local environment of the mobile ions. However, only little information has been gained concerning the conduction process in the glasses. In an attempt to at least partly overcome this problem we have applied the bond valence method to reverse Monte Carlo produced structural models of ion conducting glasses. Although we are still not able to directly elucidate the dynamical process, it has been possible to understand experimental conductivity data on a structural basis. In fact, the experimental conductivity and its associated activation energy can be predicted directly from the structural models and conduction anomalies, such as the well-known mixed alkali effect, can be understood using the bond valence approach. Here, we also discuss the possibility of exploring the conduction process in more detail by elucidating the number of available sites for the mobile ions and the dimensionality of the conduction pathways as a function of temperature.

(Some figures in this article are in colour only in the electronic version)

1. Introduction

In order to understand ion conduction in glassy electrolytes it is essential to explore the relation between conductivity and structural properties. The ionic conductivity of glasses as a function of the frequency of an applied electric field can be studied by dielectric spectroscopy, and structural information can be obtained by a wide range of techniques: mainly neutron and x-ray diffraction approaches for general information and nuclear magnetic resonance (NMR),

extended x-ray absorption fine structure (EXAFS) and vibrational spectroscopy for local information on specific parts of the structure. However, it is not straightforward to decide how all this experimental information should be used to obtain a complete 'structural picture' of the glass and it is even more difficult to understand the measured conductivity properties without having a full picture of the structure. Thus, a pure experimental approach to this problem has some clear limitations.

An alternative method for exploring the relation between structure and conductivity is to use molecular dynamics (MD) simulations; in theory this is an ideal computational method since all possible structural and dynamical information can be extracted (at least within the limited size of the system and the limited time of the simulation). The MD approach has also in practice been shown to be a very useful method for obtaining insights into the conduction mechanism and how it is related to the atomic structure [1–5]. However, unfortunately there are also drawbacks in this case. Besides the difficulty of reaching simulation times of microseconds or more, the most serious limitation is the problem of obtaining realistic interatomic model potentials between the particles in chemically complicated glasses. Since this makes it difficult to reproduce experimentally observed structural and dynamical properties of the glasses it also implies that most of the other output results are not completely correct. In many cases the errors are likely to be sufficiently small that results that are relevant for a qualitative description of the conduction process are still produced. Nevertheless, it is difficult to evaluate the correctness of the results and it would be desirable to have structural and dynamical models of the glasses that are totally consistent with all available experimental results. In the case of structural models describing the dynamics, there is so far no more accurate method than MD (or *ab initio* MD) simulations, but to reproduce experimental structural data quantitatively there is the possibility of using reverse Monte Carlo (RMC) modelling [6, 7].

The RMC method has been shown to be an excellent tool for producing three-dimensional structural models in quantitative agreement with diffraction, EXAFS and NMR data, as well as additional bonding constraints based on other experimental or chemical knowledge [8–12]. In this way it has been possible to determine the distribution and local environment of the potentially mobile ions, which is essential in order to be able to understand the conduction process. However, since the RMC method does not provide any dynamical information it is not possible to gain any direct insight into the conduction process in the glasses, without applying further analysis of the structural models. The aim of this paper is to describe such a method for elucidating the relation between structure and conductivity and for understanding experimental conductivity data on a structural basis. The tool we refer to is called 'the bond valence method' and will be described in the next section.

2. The bond valence method

The bond valence method is most widely used in crystallography to evaluate the plausibility of proposed crystal structures [13–15]. It is based on the idea that the total bond valence sum V of a M^+ ion may be expressed as

$$V = \sum_{X} s_{M^+-X}, \tag{1}$$

where the individual bond valences s_{M^+-X} for bonds to all adjacent anions X are commonly given by

$$s_{M^+-X} = \exp\left[\frac{R_0 - R_{M^+-X}}{b}\right]. \tag{2}$$

The bond valence parameters R_0 and b are deduced from a large number (typically about 100) of crystalline compounds containing the same M^+–X pairs, but having different coordination numbers and bond length distributions. In all these different environments and coordination types a monovalent cation should have a bond valence sum close to $V_{\text{ideal}} = 1$. Least squares refinements of R_0 and b are listed in [16] for a wide range of different M^+–X pairs. As for the crystalline compounds, the process of ion transport from one equilibrium site to another should follow the route which requires the lowest valence mismatch $\Delta V = |V - V_{\text{ideal}}|$, corresponding to the energetically most favourable pathway. Thus, in principle the activation energy E_σ should be directly related to ΔV. However, since our structural models are limited to about 4000 atoms and ΔV shows large variations in the structure, it is not an easy task to determine the absolutely lowest value corresponding to the experimentally measured E_σ. A simple and reliable way to quantify E_σ has been shown to be determining the 'pathway volume' for a given maximum value of ΔV [17]. This implies that ΔV has to be calculated for a hypothetical M^+ ion at each point in the structure. In practice (since the number of points in the structure would be infinite without any limitations of the resolution), the number of points was restricted by dividing the RMC produced structural models into about four million cubic volume elements with a size of about $(0.2\ \text{Å})^3$. After ΔV had been calculated for each volume element the 'pathway volume' was determined as the total volume of all volume elements having a ΔV lower than the given maximum value. The volume elements within the pathway volume were then considered to form conduction pathways for the mobile ions. To ensure that the limited grid resolution does not cause any problems we also considered volume elements where $V - V_{\text{ideal}}$ changes its sign across them as accessible for the migrating ions. If these accessible volume elements share common faces or edges they belong to the same 'pathway cluster'. Such pathway clusters will contribute to the dc conductivity only if they percolate through the structural model. The remaining restricted pathway clusters are considered to contribute only to the ac conductivity.

As mentioned above, a maximum value of ΔV has to be chosen somewhat arbitrarily, although it should be related to the experimentally determined value of E_σ for the glass and (as will be discussed further below) the mass m_{M} of the mobile ion. Obviously, the maximum value of ΔV has to be large enough to permit the formation of percolating clusters of the accessible volume elements (at least if dc conductivity is to be studied). On the other hand, if the maximum value of ΔV is too large the largest pathway cluster will be considerably larger than the real dc conduction pathways, and the nature of the bond valence pathways will be of low relevance for the conduction process. However, fortunately, the size of the largest pathway cluster increases only slightly with the chosen maximum ΔV, and the relative increase of the cluster size with increasing maximum ΔV is roughly the same for all glasses; see [17]. This means that the maximum value of ΔV has only a minor effect on the results as long as it is reasonably realistic. A problem occurs only when the same maximum ΔV is used to compare the conduction process in glasses with conductivities differing by about ten decades or more. Either the maximum ΔV will be too large for the best conducting glasses (having the lowest E_σ) or too low for the glasses with lowest conductivities (largest E_σ). However, for glasses with conductivities in the range 10^{-10}–10^{-2} S cm^{-1} the results are basically unaffected by the chosen maximum ΔV, as long as it is in the range 0.05–0.2 valence units.

3. The inclusion of a new bond valence constraint in the RMC method

The RMC method has been extensively described elsewhere [6, 7], so here we will focus on a new soft bond valence constraint, which is suitable for use for ions or atoms that do not have well-established local environments. For pure network glasses, such as SiO_2, there

is, of course, no need to use any bond valence constraint since the local environments of O and Si can be accurately defined by rigid bonding constraints with well-defined coordination numbers. For materials having ions or atoms with a distribution of both coordination numbers and interatomic distances the rigid bonding constraint approach does not work. There is the possibility in the 'standard' RMC method to use a constraint on the average coordination number, which can usually be experimentally determined with a reasonable accuracy even for, for instance, mobile metal ions in ion conducting glasses. However, the drawback of using such an average constraint is that it does not correlate the coordination number of a particular atom or ion with the bonding distances for that particular particle, as is the case in reality. To overcome this problem and obtain realistic local environments also for atoms or ions having a distribution of coordination numbers a soft bond valence constraint can be used, since that constraint modifies the expected bonding distances according to the coordination numbers so the total bond valence sum remains realistic irrespective of the coordination number.

The soft bond valence sum constraint minimizes the valence difference ΔV of each mobile M^+ ion during the procedure of fitting to the diffraction data. To determine ΔV we first had to calculate the total bond valence sum V of each mobile M^+ ion by using equations (1) and (2) with the same bond valence parameters R_0 and b as given in [16] for a wide range of different interatomic pairs. Thereafter, the average bond valence mismatch per mobile M^+ ion was calculated through

$$\langle \Delta V \rangle = \left[\sum_{M=1}^{n} |V(\mathrm{M}) - V_{\mathrm{ideal}}| \right] \Big/ n. \tag{3}$$

$\langle \Delta V \rangle$ was then minimized in the RMC modelling in the same way as the deviations between the calculated and experimentally measured structure factors were minimized, i.e. by calculating

$$\chi_i^2(V) = \langle \Delta V \rangle^2 / \sigma^2(V) \tag{4}$$

where $\sigma(V)$ is an input parameter that depends on the assumed ΔV. The value of $\chi_i^2(V)$ was thereafter added to the contributions arising from deviations between the calculated and experimentally measured structure factors and deviations from the target coordination constraints (more details about these contributions are given in [6, 7]). A random atomic move is always accepted if $\chi_{i+1}^2(\mathrm{total}) < \chi_i^2(\mathrm{total})$, and if $\chi_{i+1}^2(\mathrm{total}) > \chi_i^2(\mathrm{total})$ the move is accepted with the probability $\exp(-(\chi_{i+1}^2 - \chi_i^2)/2)$ as in the 'standard' RMC method.

The effect of this soft bond valence constraint on the structure is evident in figure 1. The figure shows how the bond valence sum distributions of Li^+ and Na^+ ions are altered when the soft bond valence constraint is included in the RMC modelling of the alkali glasses MPO_3 (M = Li, Na). As seen from figure 1 the average value of the bond valence sum $V(\mathrm{M})$ increases and the distribution gets narrower. The main reason for the increased average value is that the average coordination number increases slightly, and the reduced width is mostly due to the reduced number of M^+ ions with exceptionally low coordination numbers (<3). This implies that the numbers of structural 'defects' or unrealistic local environments of the mobile M^+ ions have been reduced by the inclusion of the bond valence constraint. However, as figure 1 indicates, it was not possible to fit the diffraction data with a strict constraint on the valence sum, i.e. a very low value of $\sigma(V)$, suggesting that the individual M^+ ions in real glasses show substantial deviations from the empirical ideal valence sum (=1 for a monovalent ion). The main reason for this is however that the RMC method produces an instantaneous picture of the structure (since the diffraction data provide such information), rather than an energy-minimized ideal structure where all vibrating atoms are located in their equilibrium positions. Thus, for a structure with all particles located at their equilibrium positions the deviations from the ideal valence sum would be considerably less. It may also be noted from figure 1 that the width of the bond valence sum distribution for Na^+ is somewhat higher than that for Li^+.

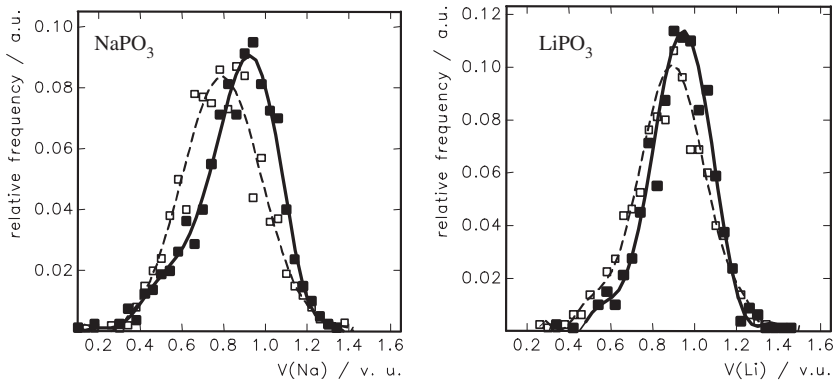

Figure 1. Bond valence sum distributions of the Li^+ or Na^+ cations in MPO_3 (M = Na, Li) glasses before (open symbols, broken curve) and after (filled symbols, solid curve) the soft bond valence constraint was included in the RMC modelling.

4. Results

4.1. Structure–conductivity correlations

As mentioned above, pathways for ion transport are assumed to be equivalent to the clusters of adjacent accessible sites, which are determined by the bond valence method for a given maximum ΔV. Percolating clusters will then represent continuous conduction pathways for the long-range ion transport giving rise to dc ionic conductivity. A few years ago we were able to show for a wide range of Ag^+ conducting glasses that the volume fraction F of the respective infinite pathway clusters is related to the experimental dc conductivity σ of the system at the temperature T of the experimental diffraction data used to build the RMC structure model [17]. We found that

$$\log(\sigma T) = A_1' \sqrt[3]{F} - B_1' \tag{5a}$$

and that the experimentally determined activation energy E_σ for ion migration is given by

$$-\left(\frac{E_\sigma}{k_B T}\right) = A_2' \sqrt[3]{F} - B_2', \tag{5b}$$

with empirical (positive) constants A_i', B_i' that depend on the chosen value of the maximum ΔV. Later [18] these linear relations were generalized to mobile ions of other types, such as alkali ions. It was found that the separate structure–conductivity correlations observed for each kind of mobile ion (see figure 2(a)) can be combined to a unified empirical relationship by employing the square root of the cation mass m as a scaling factor (see figure 2(b)). Thus, equations (5*a*) and (5*b*) are then modified to

$$\log(\sigma T \sqrt{m}) = A_1 \sqrt[3]{F\sqrt{m}} - B_1 \tag{6a}$$

and

$$-\left(\frac{E_\sigma}{k_B T}\right) = A_2 \sqrt[3]{F\sqrt{m}} - B_2. \tag{6b}$$

The reason for the mass scaling of the experimental conductivity is that the attempt frequency for an ionic jump is approximately proportional to the inverse square root of the cation mass. The mass scaling of the pathway volume fraction F is less obvious and is discussed in detail in [18]. Briefly, one can say that this scaling is performed because a higher cation mass favours

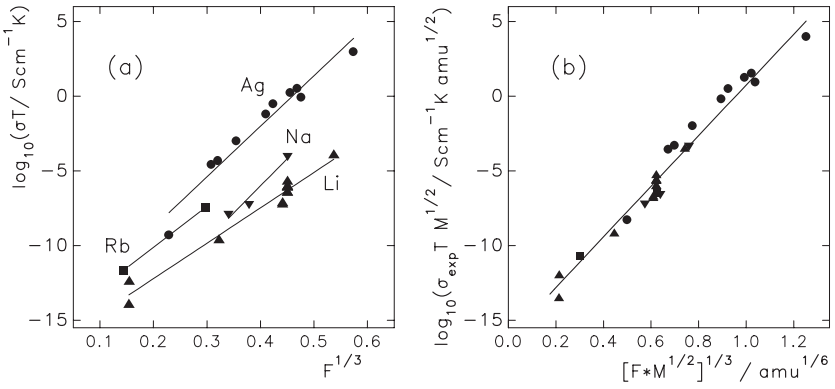

Figure 2. Correlations between the cube root of the pathway volume fraction F and the experimental conductivity σ without mass scaling (a) and with mass scaling ($M^{1/2}$) (b) for the ion conducting glasses MPO_3 (M = Li, Na, Rb, Li_xNa_{1-x}, Li_xRb_{1-x}); $(MCl)_x$–M_2O–$2B_2O_3$ ($x = 0$, 1; M = Li, Na) as well as for a wide range of Ag^+ conducting glasses (for a list of Ag glasses investigated see [17]).

the decoupling of the motions of the cation and glass matrix; i.e. the connection between the activation energy scale and the bond valence mismatch scale is mass dependent. The close relation between F and the experimentally determined conductivity is an important observation since it enables us to predict the conductivity directly from the structure models, and thereby to understand why certain structural properties are beneficial to the conductivity.

The local environment of the mobile ions located in the conduction pathways has also been investigated in some detail. The most interesting results from these studies were shown for AgI-doped fast ion conducting glasses. It has been suggested [19] that the high ionic conductivity in highly AgI-doped glasses is due to a process of conduction through AgI clusters with a structure similar to that of the high temperature α-phase of crystalline AgI. However, our bond valence analysis shows clearly that the majority of the Ag^+ ions located in the long-range conduction pathways have mixed oxide/iodide coordination, and the pathways including only iodide coordinated sites are restricted to very local regions of a few Å [17]. Thus, sites with a high oxide coordination are important for the long-range diffusivity.

4.2. The mixed alkali effect

Other important results have been obtained for the mixed alkali glass system $Li_xRb_{1-x}PO_3$ ($x = 0, 0.25, 0.5, 0.75$ and 1), which was studied with the aim of achieving an understanding of the mixed alkali effect (MAE) in glasses. As indicated in figure 2(b) (see also figure 1 in [20]), the experimentally observed drop in conductivity (by more than six orders of magnitude compared to that for the single-alkali glasses) for an intermediate composition ($x = 0.5$) is reproduced within the experimental errors. This implies that the MAE can be understood on a purely structural basis. A detailed analysis of the conduction pathways showed that these were of low dimensionality (<2) and distinctly different for the two kinds of alkali ions. Since the Li^+ and Rb^+ ions are randomly mixed in all the conduction pathways this results in a highly effective blocking of Li pathways by Rb^+ ions and vice versa. This blocking effect was found to be the main reason for the MAE in glasses.

Similar findings are observed for the mixed alkali glass system $Li_xNa_{1-x}PO_3$ ($x = 0$, 0.5 and 1). The structure of the $Li_{0.5}Na_{0.5}PO_3$ glass is shown in figure 3, and from comparing with figure 2 in [20] it is evident that the structure of this glass is very similar to that of

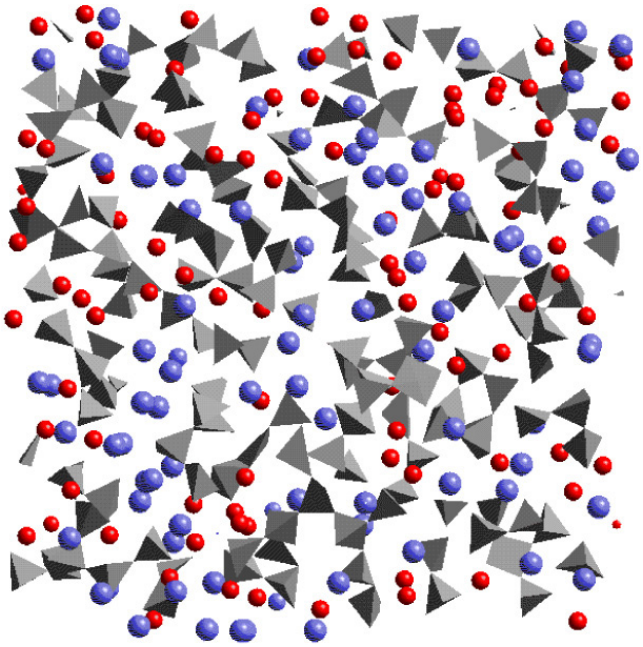

Figure 3. A 8 Å thick slice of the RMC produced structural model of the $Li_{0.5}Na_{0.5}PO_3$ glass. Small spheres refer to lithium, larger spheres to Na and PO_4 groups are shown as tetrahedra.

$Li_{0.5}Rb_{0.5}PO_3$. However, the drop in conductivity, relative to those for the two single-alkali glasses, is slightly lower than for the $Li_{0.5}Rb_{0.5}PO_3$ glass due to the smaller size difference between Li^+ and Na^+ compared to Li^+ and Rb^+. The bond valence mismatch for a hypothetical Li^+ ion on a site adapted to Na^+ (0.47 vu) is significantly smaller than that on a site adapted to Rb^+ (0.76 vu), which both increases the (still very low) probability of jumps on dissimilar sites and enhances the mobility of dissimilar 'blocking' ions. Thereby, the blocking effect becomes slightly less effective in the $Li_xNa_{1-x}PO_3$ glass. Figure 4 shows the pathway volumes of Li^+ and Na^+ in the three glass compositions, as well as the Li^+ pathways in $Li_{0.5}Na_{0.5}PO_3$ and those regions that are blocked by Na^+ ions but otherwise would have a matching bond valence and therefore have provided conduction pathways for the Li^+ ions. Figure 5 compares the predictions for room temperature conductivity and activation energies of $Li_xNa_{1-x}PO_3$ glasses from the pathway volume fraction (see figure 2) with experimental data extracted from graphs in the literature [21, 22]. In the case of conductivities it was necessary to extrapolate room temperature data from the reported measurements at higher temperatures. From figure 5 it is evident that the blocking effect is still, by far, the dominant contribution to the conductivity drop, but that the conductivity is also reduced due to the structure of $Li_{0.5}Na_{0.5}PO_3$ being less adapted to Li^+ ions than in $LiPO_3$. Due to the smaller differences in cation size, preferred coordination number etc, the latter contribution to the MAE is equally smaller than for the $Li_{0.5}Rb_{0.5}PO_3$ glass.

From the idea that the bond valence mismatch threshold $|\Delta V|$ used in determining the bond valence pathway should be related to the kinetic energy of the mobile cations, a comparison of the pathways found for a series of different valence mismatch thresholds should provide further insight into the effect of temperature on the conductivity of glasses. Figure 6 illustrates the determination of the local pathway dimensionality for Li^+ ions in $Li_{0.5}Na_{0.5}PO_3$ using different

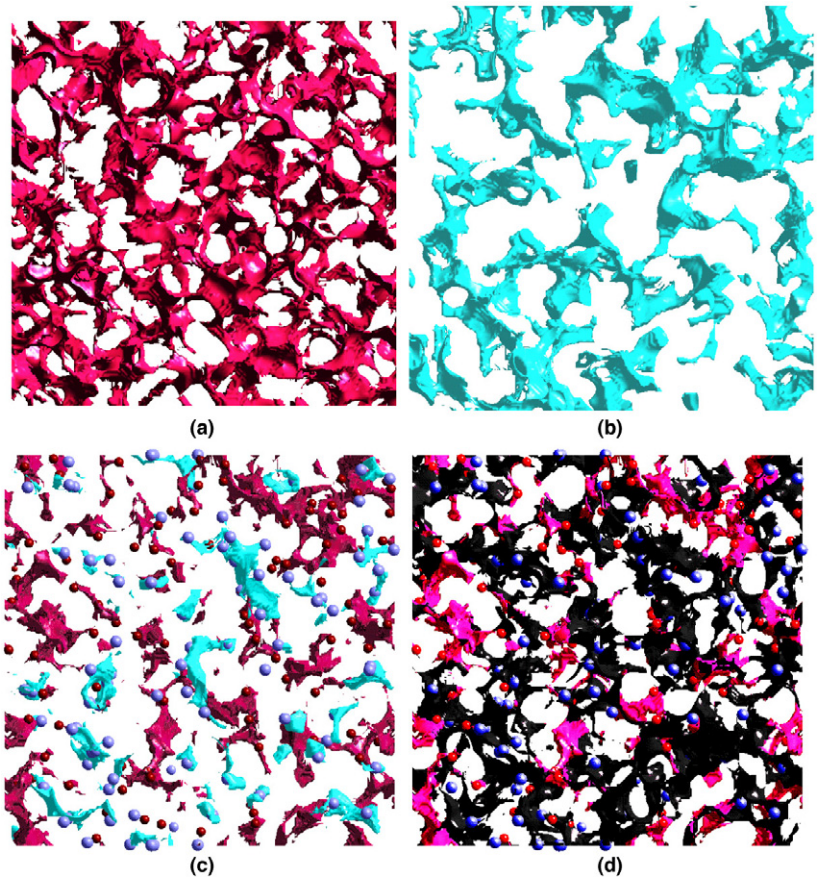

Figure 4. 8 Å thick slices through the ion conduction pathways (isosurfaces of bond valence mismatch $\Delta V \leqslant 0.2$ vu) for Li^+ (dark) and Na^+ (light) in $Li_xNa_{1-x}PO_3$: (a) Li^+ pathways in $LiPO_3$; (b) Na^+ pathways in $NaPO_3$; (c) Li and Na pathways in the mixed alkali system $Li_{0.5}Na_{0.5}PO_3$; (d) Li pathways (light) in $Li_{0.5}Na_{0.5}PO_3$ and regions that are blocked by Na^+ ions but have a matching Li bond valence (dark) and therefore would otherwise belong to the Li^+ conduction pathways. In (c) and (d) the Li^+ (Na^+) positions from the RMC model are marked by small (large) spheres.

values of $|\Delta V|$ and disregarding the blocking by Na^+. The observed slight increase in the pathway dimensionality with $|\Delta V|$ and hence with temperature suggests that for mixed alkali systems the blocking of pathways by unlike cations will become less effective, in qualitative agreement with the less pronounced mixed alkali effect observed at elevated temperatures. Figure 6 also illustrates that the slope changes to 3 for longer length scales reflecting the three-dimensional cross-linkage of the locally low dimensional paths (for the range of ΔV values shown in figure 6). Both the difference between the low dimensional short-range and three-dimensional long-range characteristics of the pathway network and the distribution of the local dimensionalities might affect the frequency dependence of the ac conductivity.

4.3. The transport mechanism

While the mechanism of ion transport in most crystalline solid electrolytes appears to be well understood in terms of interstitial, interstitialcy or vacancy mechanisms, there is a continuing

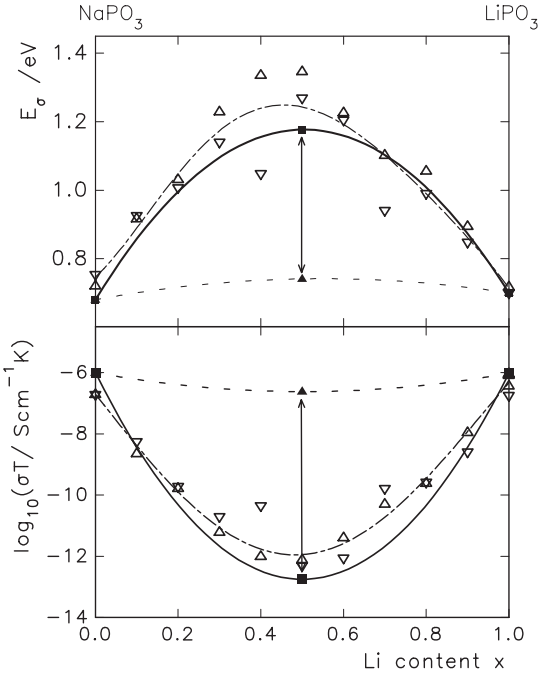

Figure 5. Activation energy and conductivity versus composition for the glass system $Li_xNa_{1-x}PO_3$. Open symbols are experimental data points taken from the literature (△: [21]; ▽: [22]), and filled squares (triangles) correspond to the values predicted from the pathway volume fractions F in $Li_{0.5}Na_{0.5}PO_3$ if the effect of blocking by unlike mobile cations is taken into account (neglected) in the calculations. Curves represent polynomial fits as a guide to the eye. The vertical arrows mark the dominant portions of the MAE that can be attributed to the blocking by unlike cations.

debate on whether comparable conduction mechanisms can occur in glasses. In line with more general considerations, as regards whether cation sites in a glass could be classified as interstitials at all [23–26], the existence of percolating low bond valence mismatch pathways revealed in our previous studies seems to favour vacancy-type mechanisms. To gain a deeper insight into the transport mechanism, it appears indispensable to count (and classify) all sites that a mobile ion can visit in a given glass structure. Such attempts have been undertaken previously on the basis of molecular dynamics trajectories for a number of glass systems using different routines to identify suitable sites [23, 27]. The basic approach for identifying sites which have actually been occupied by the mobile ions for a certain while results in the fundamental uncertainty that the number of sites depends on the simulation period. This may become a relevant drawback for systems with low cation mobilities.

On the other hand, the detection of equilibrium sites using the bond valence method presented here for RMC models of various metaphosphate glasses MPO_3 (where M = Li^+, Na^+, Rb^+, Ag^+) and AgI-doped $AgPO_3$ may rather be (approximately) identified with an analysis of the complete energy landscape for the modelled local structure snapshot at a certain instant. This method should therefore yield a complete picture for that instant, but of course lacks the information on time evolution.

For each of the systems the starting point is again the identification of ‘accessible’ sites within the RMC structure model. To account for the above-mentioned mass dependence of the conversion between activation energy and the bond valence mismatch we employed a valence

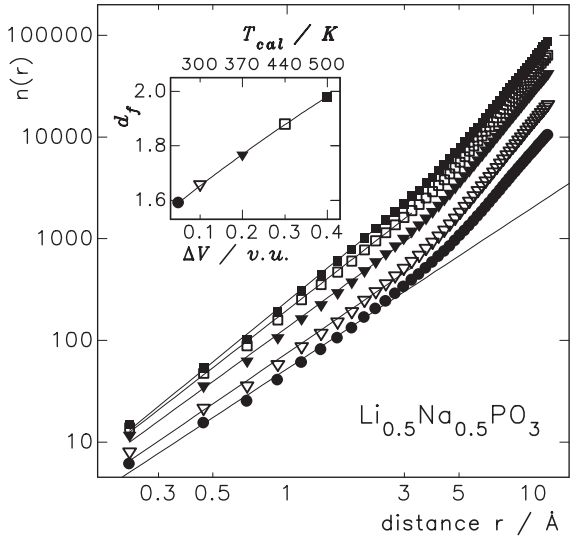

Figure 6. Correlations between the average number $n(r)$ of sites in the infinite pathway cluster up to a distance r from a Li pathway cluster site in the $Li_{0.5}Na_{0.5}PO_3$ glass. Different symbols indicate different valence mismatch thresholds ΔV(Li) in the range 0.05–0.4 vu. The variation of the slope d_f (representing the dimensionality of the pathways on these local length scales) is shown in the inset as a function of ΔV(Li) as well as of a calculated temperature $T_{\rm cal}$ derived empirically from the bond valence mismatch (assuming that ΔV(Li) = 0.1 vu corresponds to $T = 300$ K).

mismatch threshold of 0.02 vu/amu$^{1/2}$ $\times$ $m_{\rm M}^{1/2}$ (amu = atomic mass unit), which leads to valence mismatch thresholds ranging from 0.05 to 0.2 vu. Due to the limited grid resolution, using much smaller valence mismatch thresholds would bear the danger of missing some of the local bond valence sum minima.

As discussed in connection with the pathway cluster analysis the condition of a sufficiently low bond valence mismatch will not produce individual sites but a continuous network of sites with only marginal differences among their bond valence mismatches. Therefore it is necessary to identify further criteria that permit one to locate the most suitable sites within the pathways. The bond valence approach suggests that if a cation can reach the appropriate bond valence sum in various ways it will prefer the coordination that leads to the most uniform distribution of individual bond valences (equal valence rule [13, 14]). Together with the knowledge that the coordination number (CN) for equilibrium sites of a certain cation will vary only over a limited range, this can be used to resolve the pathways into equilibrium sites.

Here we classify anions as coordinating a central cation if the cation–anion distance corresponds to an individual bond valence that is $\geqslant$0.075 valence units (vu). It may be noted here that this minimum bond valence threshold is by intention almost twice the one that is normally considered to be appropriate (0.04 vu; see e.g. [14]) to eliminate strongly distorted coordinations. A survey of the cation coordinations in sets of well-determined, fully ordered inorganic crystal structures extracted from the Inorganic Crystal Structure Database [28] using this CN definition demonstrates that the ranges of preferred CN for Li^+, Na^+, Rb^+ and Ag^+ in oxides are then 4–6, 4–6, 4–8 and 2–6, respectively (see table 1). Only sites that would lead to a CN within this range are counted as equilibrium sites. As none of the cations investigated tends to form multiple bonds, sites that would lead to individual bond valences that are significantly $>1/4$ for the alkali glasses or $>1/2$ for the Ag glass are also eliminated.

Table 1. Distribution of coordination numbers (CN) in fully ordered crystal structures containing O^{2-} as the only type of anion. Crystal structures have been extracted from the ICSD database [28].

Atom pair	Cation environments	Distance threshold (Å)	Relative frequency of cation coordination numbers (%) CN							
			2	3	4	5	6	7	8	⩾9
Li–O	112	2.51	—	—	**46**	**20**	**34**	—	—	—
Na–O	1133	2.815	0	2	**20**	**20**	**47**	6	4	0
Rb–O	352	3.156	1	6	**13**	**16**	**28**	**16**	**13**	4
Ag–O	341	2.81	**24**	**13**	**29**	**14**	**14**	2	3	0

Table 2. The number $n_{\text{eq.s.cl}}$ and size of 'equilibrium site clusters' in the RMC models of glass structures investigated. Values for $n_{\text{eq.s.cl}}$ in Ag^+ conducting glasses are given in brackets, since these clusters are large enough to be occupied by several Ag^+ ions simultaneously.

	$\lvert\Delta V\rvert$ (vu)	n_M[a]	$n_{\text{eq.s.cl}}$[b]	Average size of eq. site clusters/ grid elements	Average size of eq. site clusters (Å^3)
$LiPO_3$	0.053	800	2506	7.2	0.08
$NaPO_3$	0.096	800	2154	12.2	0.16
$RbPO_3$	0.184	800	1755	8.7	0.15
$Li_{0.5}Na_{0.5}PO_3$(Li)	0.053	400	1533	5.84	0.07
$Li_{0.5}Na_{0.5}PO_3$(Na)	0.096	400	981	13.68	0.16
$AgPO_3$	0.208	768	(233)	755	9.76
$10AgI–90AgPO_3$	0.208	853	(441)	366	5.21
$30AgI–70AgPO_3$	0.208	1000	(454)	436	7.15
$50AgI–50AgPO_3$	0.208	1200	(331)	788	15.0

[a] n_M: number of M^+ cations in the RMC model.
[b] $n_{\text{eq.s.cl}}$: number of equilibrium site clusters according to the definition used in the text.

In the case of $LiPO_3$, '*equilibrium site clusters*' are thus defined as clusters of grid points within the (hypothetical Li site) RMC structure model that exhibit a bond valence sum mismatch that is <0.02 vu$/\sqrt{\text{amu}} \times \sqrt{6.941\ \text{amu}} = 0.053$ vu, a coordination number in the range $4 \leqslant \text{CN} \leqslant 6$ and a closest Li–O distance that is >1.8 Å.

For the alkali phosphate glasses these criteria seem to be adequate for localizing clusters of equilibrium sites that are sufficiently small (about 10 grid sites or about $(0.5\ \text{Å})^3$ on average; see table 2) that they can only be occupied by a single cation. Due to the tendency of silver ions to occur in low CN configurations (which imposes the considerably less strict coordination number constraint $2 \leqslant \text{CN} \leqslant 6$), the same formalism leads to much larger 'equilibrium site clusters' in silver ion conducting glasses that may be occupied by several Ag^+ at the same time, which will tend to facilitate the occurrence of correlated ion jumps in the silver ion conducting glasses.

To ensure that the modelled site clusters are related to the cation positions of the RMC model we have also determined the distance of the M sites from the 'equilibrium clusters'. The typical distance seems to be well within the range for a hopping distance (cf figure 7). For the alkali metaphosphate glasses the average distance d is close to the exclusion radius of the respective mobile cation. (It may be noted, however, that the values of d for Li^+ and Na^+ in $Li_{0.5}Na_{0.5}PO_3$ are about 40% higher than for the same cation in the respective single-alkali glass.) Figure 7 also illustrates that the probability for an Ag^+ to occupy sites within these clusters at the modelled 'instant' is much higher because of the much more extended 'equilibrium site clusters' in the $AgPO_3$ and $AgI–AgPO_3$ glasses.

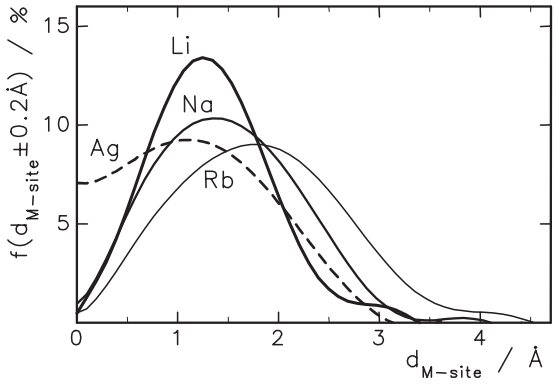

Figure 7. The frequency $f(d)$ of distances $d_{\mathrm{M\,site}}$ between the modelled M^+ positions in the RMC models of MPO_3 glasses (M = Li, Na, Rb, Ag) and the closest equilibrium site (according to the definition explained in the text).

The formalism described so far does not take into account whether all these equilibrium site clusters can be occupied simultaneously. Effectively the criteria will tend to result in a considerable number of closely neighbouring clusters and thereby overestimate the number of relevant sites. The number of those sites n_{site} that have a suitable minimum distance from each other and therefore can be occupied independently is assessed by running systematically through all sites. Wherever an accessible site within an equilibrium site cluster is identified, all surrounding sites up to a distance of $2r_{\mathrm{M}}$ are eliminated before continuing the loop.

The appropriate M–M exclusion distances $2r_{\mathrm{M}}$ can again be assessed by comparison with sets of reliable reference crystal structures that contain short M–M distances (extracted from the ICSD [28]). The exclusion radii were then approximated by the zero point of the linear extrapolation of the frequency distribution of r_{M}, shown in figure 8. The resulting exclusion radii $r_{\mathrm{Li}} = 1.17$ Å, $r_{\mathrm{Na}} = r_{\mathrm{Ag}} = 1.38$ Å for Na and Ag and $r_{\mathrm{Rb}} = 1.85$ Å are as expected slightly smaller than the respective metallic radii and consistent with the minimum distance criteria employed in the RMC modelling of the systems investigated. Although unrealistically short cation–cation distances have been eliminated from the reference data, these exclusion radii should be taken as minimum values (because the zero point will be biased by some too short cation–cation distances that arise from statistical errors in the reference data) and the resulting number of sites may thus be slightly overestimated.

Table 3 summarizes the resulting absolute numbers of sites that can be occupied simultaneously in each of the glass structure models investigated. Due to the numerous assumptions involved, the given ratios of sites per ion can certainly only be taken as approximate values. It has however been checked that the total number of sites varies only slightly with these parameters (e.g. $n_{\mathrm{sites}}/n_{\mathrm{Ag}}$ for $AgPO_3$ changes from 1.25–1.34 if the valence mismatch threshold is varied over the range 0.015–$0.025 \times m_{\mathrm{Ag}}^{1/2}$ (vu)). A comparison of the different alkali metaphosphate glass structure models suggests that only the motion of Li^+ in $LiPO_3$ involves significantly more sites than ions. With increasing size and softness of the cations the number of sites is considerably reduced (although the valence mismatch threshold is increased by the same order). In the case of $RbPO_3$ the number of sites that qualify as equilibrium sites at the modelled instant is even somewhat lower than the total number of Rb^+, indicating that a notable fraction of the Rb^+ is locked in less favourable positions. These positions may then act as sources or sinks of mobile cations. From the pronounced differences between the sites/cation ratios for the different alkali phosphate glasses it may be tentatively concluded that

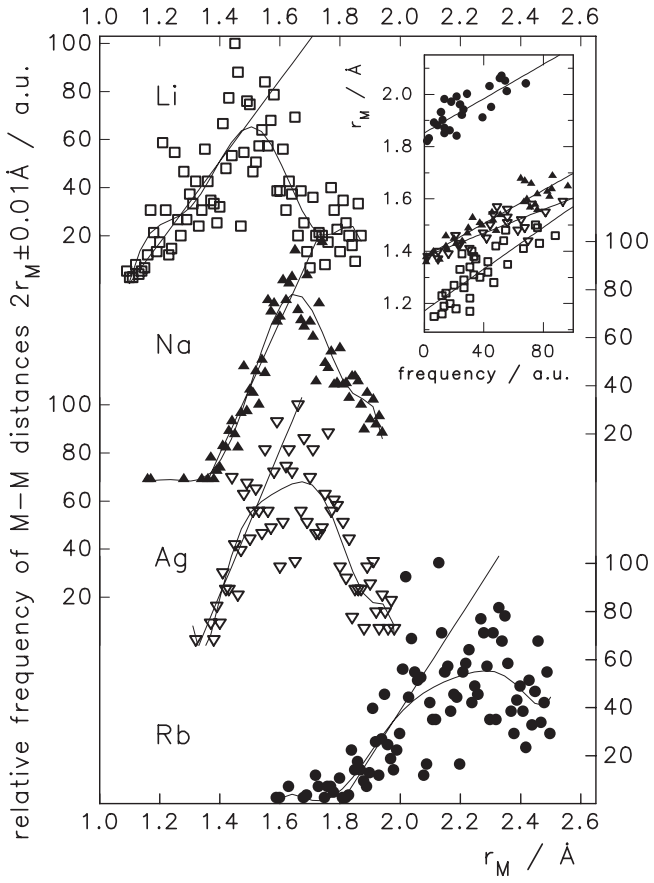

Figure 8. The relative frequency of short M–M distances (M = Li, Na, Rb, Ag) in well-determined inorganic crystal structures from the ICSD database. The zero point of the displayed linear extrapolations yields the chosen exclusion radii. The inset shows a radius versus relative frequency diagram of the data included in the linear regression.

(as for crystalline ionic conductors) there will not be a unique ion transport mechanism for all glass systems.

In the system AgI–$AgPO_3$ the number of sites increases only slightly with the dopant concentration so this increase cannot explain the drastic increase of the conductivity with the dopant concentration. Moreover, the extended 'equilibrium site clusters' may be taken as an indication that the concept of well-localized cation sites is less suitable for the silver ion conducting glasses than for the alkali glasses or other main group cation glasses.

5. Concluding remarks

The investigations discussed in the previous section demonstrate that incorporation of bond valence constraints into the reverse Monte Carlo modelling algorithm enhances the chemical plausibility of RMC glass structure models. The analysis of the energy landscape for mobile ions in terms of the bond valence approach provides a valuable tool for promoting the understanding of ion transport in glasses. Besides the predictive power of the observed

Table 3. The number of equilibrium cation sites n_{sites} that can be occupied simultaneously within the RMC models of the metaphosphate glasses investigated.

	r_M (Å)[a]	n_M[b]	n_{sites}[c]	n_{sites}/n_M
$LiPO_3$	1.17	800	1173	1.47
$NaPO_3$	1.38	800	874	1.09
$RbPO_3$	1.85	800	558	0.70
$Li_{0.5}Na_{0.5}PO_3$(Li)	1.17	400	767	1.92
$Li_{0.5}Na_{0.5}PO_3$(Na)	1.38	400	464	1.16
$AgPO_3$	1.38	768	993	1.29
10AgI–90$AgPO_3$	1.38	853	1178	1.38
30AgI–70$AgPO_3$	1.38	1000	1469	1.47
50AgI–50$AgPO_3$	1.38	1200	1794	1.50

[a] The exclusion radius of cation M.
[b] n_M: number of M^+ cations in the RMC model.
[c] The number of sites in the RMC model that can be occupied simultaneously (taking into account the mutual exclusion of like cations).

correlation between structure and conductivity, various recent molecular dynamics simulations (mainly on silicate glasses) have confirmed independently that at temperatures sufficiently below the glass transition temperature cation transport pathways persist over periods that are long enough (compared to the timescale of individual jump processes) to control the ion transport [29–32]. The possibility of characterizing these pathways in terms of their dimensionality and the number of equilibrium sites should help to classify ion transport mechanisms in glasses. Due to the comparatively small computational effort it should be possible to analyse RMC models of glasses routinely by this technique, which should finally help to distinguish more clearly between universal transport properties in glasses and peculiarities of individual systems.

Although our analysis of the static RMC models grants even some qualitative conclusions about the frequency and temperature dependence of the conductivity, a consistent quantitative characterization and understanding of all aspects of motion in glasses can only be expected from an approach that utilizes (preferably experimental) information on both the space and time domain.

Acknowledgments

JS is a Royal Swedish Academy of Sciences Research Fellow supported by a grant from the Knut and Alice Wallenberg Foundation. Financial support to JS from the Swedish Foundation for Strategic Research and to SA from the Deutsche Forschungsgemeinschaft is gratefully acknowledged.

References

[1] Huang C and Cormack A N 1992 *J. Mater. Chem.* **2** 281
[2] Cormack A N 1998 *J. Non-Cryst. Solids* **232–234** 188
[3] Balasubramanian S and Rao K J 1995 *J. Non-Cryst. Solids* **181** 157
[4] Habasaki J, Okada I and Hiwatari Y 1996 *J. Non-Cryst. Solids* **208** 181
[5] Habasaki J and Hiwatari Y 1999 *Phys. Rev.* B **59** 6962
[6] McGreevy R L 1995 *Nucl. Instrum. Methods Phys. Res.* A **354** 1
[7] McGreevy R L 2001 *J. Phys.: Condens. Matter* **13** R877
[8] Keen D A and McGreevy R L 1990 *Nature* **344** 423

[9] Wicks J, Börjesson L, McGreevy R L, Howells W S and Bushnell-Wye G 1995 *Phys. Rev. Lett.* **74** 726
[10] Swenson J, Börjesson L, McGreevy R L and Howells W S 1997 *Phys. Rev.* B **55** 11236
[11] Swenson J, McGreevy R L, Börjesson L, Wicks J D and Howells W S 1996 *J. Phys.: Condens. Matter* **8** 3545
[12] Swenson J, McGreevy R L, Börjesson L and Wicks J D 1998 *Solid State Ion.* **105** 55
[13] Brown I D 2002 *The Chemical Bond in Inorganic Chemistry—the Bond Valence Model* (Oxford: Oxford University Press)
[14] Brown I D 1997 *Acta Crystallogr.* B **53** 381
Brown I D 1992 *Acta Crystallogr.* B **48** 553
[15] Urusov V S 1995 *Acta Crystallogr.* B **51** 641
[16] Adams S 2001 *Acta Crystallogr.* B **57** 278
Adams S 2003 *softBV Database* http://kristall.uni-mki.gwdg.de/softBV/
[17] Adams S and Swenson J 2000 *Phys. Rev. Lett.* **84** 4144–7
Adams S and Swenson J 2000 *Phys. Rev.* B **63** 054201
[18] Adams S and Swenson J 2002 *Phys. Chem. Chem. Phys.* **4** 3179
[19] Rousselot C, Malugani J P, Mercier R, Tachez M, Chieux P, Pappin A J and Ingram M D 1995 *Solid State Ion.* **78** 211
[20] Swenson J and Adams S 2003 *Phys. Rev. Lett.* **90** 155507
[21] Bandaranayake P W S K, Imrie C T and Ingram M D 2002 *Phys. Chem. Chem. Phys.* **4** 3203
[22] Chen R, Yang R, Durand B, Pradel A and Ribes M 1992 *Solid State Ion.* **53–56** 1194
[23] Cormack A N, Du J and Zeitler T R 2002 *Phys. Chem. Chem. Phys.* **4** 3193
[24] Ingram M D, Imrie C T, Konidakis I and Voss S 2004 *Phys. Chem. Chem. Phys.* **6** 3659
[25] Schober H R 1998 *Phys. Rev. Lett.* **88** 145901
[26] Cordes H and Baranovskii S D 2000 *Phys. Status Solidi* b **218** 133
[27] Lammert H, Kunow M and Heuer A 2003 *Phys. Rev. Lett.* **90** 215901
[28] 1997 *Inorganic Crystal Structure Database ICSD* Fachinformationszentrum Karlsruhe, Germany
[29] Jund P, Kob W and Jullien R 2001 *Phys. Rev.* B **64** 134303
[30] Horbach J, Kob W and Binder K 2001 *Chem. Geol.* **174** 87
[31] Yuan X and Cormack A N 2003 *J. Non-Cryst. Solids* **319** 31
[32] Adams S and Swenson J 2004 *Solid State Ion.* **175** 665